ISBN: 978-3-95450-225-7 ISSN: 2673-5571 doi:10.18429/JACoW-HB2021-MOP12

UNDERSTANDING OF THE CERN-SPS HORIZONTAL INSTABILITY WITH MULTIPLE BUNCHES

C. Zannini*, H. Bartosik, M. Carlà[1], L. Carver[2], K. Li, E. Métral, G. Rumolo, B. Salvant, M. Schenk
CERN, 1211 Geneva, Switzerland
[1]now at ALBA, Barcelona, Spain
[2]now at ESRF, Grenoble, France

Abstract

At the end of 2018, an instability with multiple bunches has been consistently observed during high intensity studies at the CERN-SPS. This instability could be a significant limitation to achieve the bunch intensity expected after the LHC Injector Upgrade (LIU). Therefore, a deep understanding of the phenomena is essential to identify the best mitigation strategy. Extensive simulation studies have been performed to explore the consistency of the current SPS model, give a possible interpretation of the instability mechanism and outline some possible cures.

INTRODUCTION

Major modifications of the CERN-SPS took place during the Long Shutdown 2 (LS2) in the framework of the LHC injectors upgrade project (LIU) [1–3]. In particular, the RF system has been modified with the aim of providing the necessary RF power for compensation of beam loading, which was limiting the acceleration of LHC beams to an intensity of about 1.3×10^{11} protons per bunch (ppb) before the upgrade. The LIU upgrades of the RF system, together with the longitudinal impedance reduction, are expected to enable the acceleration of the future LHC beams to reach the target intensity of 2.3×10^{11} ppb at the CERN-SPS extraction. While such high intensity beams could not be accelerated before the upgrade, they could already be studied at injection energy. After a short description of measurement observations this paper summarises the simulation studies performed to build an understanding of the horizontal instability experienced at injection energy with high intensity LHC beams.

INSTABILITY MEASUREMENTS

During the 2015 scrubbing campaign with high intensity LHC beams (about 2.0×10^{11} ppb), a horizontal instability affecting the third and fourth batch of trains of 72 bunches was observed. Stabilization was possible with high chromaticity and octupoles.

Since 2017, an increased transverse damper gain at high frequency was available, but high chromaticity was still needed to stabilise the beam. If the chromaticity is not high enough, the unstable bunches exhibit head-tail motion as revealed by measurements with the SPS head-tail monitor. In particular, oscillation patterns of mode 1 were observed for horizontal normalised chromaticity ($\xi = Q'/Q$) settings of $0.1 \leq \xi_H \leq 0.3$ and mode 2 for $0.3 \leq \xi_H \leq 0.5$. A mode 3 pattern has also been observed for $\xi_H \approx 0.5$.

At the end of 2018, dedicated measurements were performed to further characterise the instability and test some possible cures. Four batches of 48 bunches were used for these studies. No instability was observed for lower number of batches and bunch intensity up to 2.0×10^{11} ppb. The horizontal chromaticity was kept high (normalised chromaticity of $\xi_H \approx 0.5$) for the injection of the first three batches but lowered to $\xi_H \approx 0.05$ just before the injection of the fourth batch while the transverse damper was on during the entire cycle. The octupoles were adjusted in order to compensate the horizontal detuning with amplitude due to residual non-linearities of the machine (setting of kLOF = -0.2 m^{-4}).

With the operational batch spacing of 200 ns the intensity threshold of the instability was found to be 1.8×10^{11} ppb. Figure 1 (top) shows an example of the intensity evolution along the SPS injection plateau for two different chromaticity settings. Instability starts from the last batch and extends to the other batches for lower chromaticity. Bunches in the last batch exhibit significant losses in the top plot, while for lower chromaticity (bottom plot), the instability clearly extends to the second and third batch. The growth times associated to this instability are in the order of 100 turns, as observed from the head-tail monitor acquisitions or from the turn-by-turn data of the transverse damper pickups. However, their exact value strongly depends on the damper settings. The damper, which does not have enough bandwidth to suppress the mode 1-2 head-tail instability, can, however, significantly modify the growth rates of the instability. Depending on damper settings, a variation of the instability growth rates up to a factor of three has been observed. The instability growth rates versus chromaticity have been measured and will be compared with the mode expectations in the next section.

The effect of batch spacing on the instability was also studied by varying the gap between batches in steps of 50 ns. Fewer bunches are affected by the instability when increasing the batch spacing and no instability was observed for a batch spacing larger than 500 ns.

Finally, measurements of the stability limit as a function of chromaticity and octupole settings were performed. As before, four batches of 48 bunches were injected, where the chromaticity was kept high for the injection of the first three batches and then lowered just before the injection of the fourth batch. Figure 2 shows the obtained stability limits for an intensity of about 1.8×10^{11} ppb at injection. Positive

* carlo.zannini@cern.ch

ISBN: 978-3-95450-225-7 ISSN: 2673-5571 doi:10.18429/JACoW-HB2021-MOP12

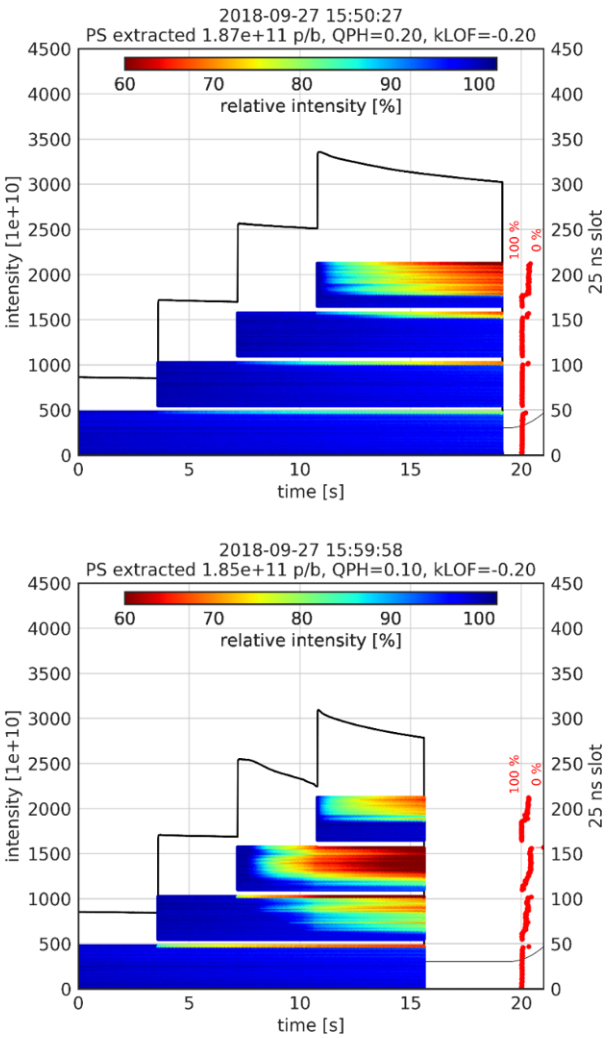

Figure 1: Intensity evolution along the SPS flat bottom for $\xi_H = 0.2$ (top) and $\xi_H = 0.1$ (bottom). In both cases, the black line indicates the total intensity and the colour indicates the relative bunch intensity. The bunch slots are indicated on the scale on the right.

values of the octupole knob are not shown as they resulted in worse beam stability.

As expected, the instability becomes more critical with higher intensity. Thus, higher octupole strength and/or higher chromaticity is needed to stabilize the beam. Stabilization was tested up to 2.1×10^{11} ppb. Therefore, there is a large range of unexplored intensities to reach the target LIU intensity of 2.6×10^{11} ppb at injection energy. A good understanding of the instability is fundamental during the intensity rump-up in order to put in place the appropriate stabilization strategy in the unexplored range of intensities.

UNDERSTANDING OF THE INSTABILITY

A theoretical analysis based on the Sacherer theory [4] has been performed to build a qualitative understanding of

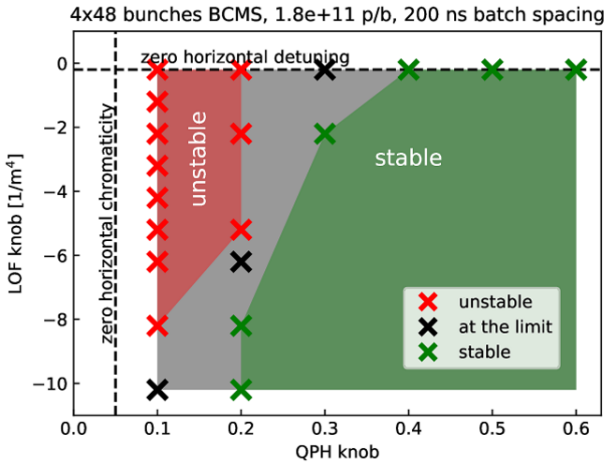

Figure 2: Measured horizontal beam stability for different chromaticity and octupole settings, where the QPH knob controls the normalised horizontal chromaticity ξ_H and the LOF knob controls the normalised octupole strength. The values for zero chromaticity and no amplitude detuning are indicated by dashed lines. The markers indicate unstable (red), stable (green) and settings where some shots were stable and some unstable (black) as obtained from about 5 shots per setting.

the instability, with an advanced macro-particle simulation model used for more quantitative analysis.

Analysis with Sacherer Theory

The effect on beam dynamics can be qualitatively assessed using the concept of effective impedance. For bunched beams the impedance is sampled at an infinite number of discrete frequencies given by the mode spectrum. An "effective coupling impedance" can then be defined as the sum over the product of the coupling impedance and the normalized spectral density. The "effective coupling impedance" is required for the calculation of both longitudinal and transverse complex tune shifts of bunched beam and can be defined in the transverse plane as [5–7]:

$$(Z_\perp)_{\text{eff}} = \frac{\sum_{p=-\infty}^{p=\infty} Z_\perp\left(\omega' + \omega_\beta\right) h_l\left(\omega' + \omega_\beta - \omega_\xi\right)}{\sum_{p=-\infty}^{p=\infty} h_l\left(\omega' + \omega_\beta - \omega_\xi\right)} . \quad (1)$$

Here $h_l(\omega)$ is the power spectral density, ω_β is the betatron angular frequency, ω_ξ is the chromatic frequency shift and $\omega' = \omega_0 p + l\omega_s$ where ω_0 is the revolution angular frequency, ω_s is the synchrotron frequency and l determines the type of oscillations (the case $l = 0$ describes the mode 0 head-tail instability). For a Gaussian bunch, $h_l(\omega)$ can be written as:

$$h_l(\omega) = \left(\frac{\omega\sigma_z}{c}\right)^{2l} e^{-\frac{\omega^2\sigma_z^2}{c^2}} , \quad (2)$$

ISBN: 978-3-95450-225-7 ISSN: 2673-5571 doi:10.18429/JACoW-HB2021-MOP12

where σ_z is the standard deviation of the Gaussian bunch profile (root mean square (RMS) bunch-length) and c is the speed of light in vacuum. The real and the imaginary parts of the "effective impedance" give the growth rate and the frequency shift of the mode under consideration, respectively [7–10]. If the real part of $(Z_\perp)_{\text{eff}}$ is negative, the beam can become unstable. The real part of the transverse impedance is an odd function of frequency. Therefore, for the mode $l = 0$, simply assuming that the impedance is positive for positive frequencies leads to the conclusion that this mode would be stable for positive spectral shift and unstable for negative spectral shift (see Fig. 3). The situation is different if we consider higher mode numbers. For a given chromatic shift the sign of the effective impedance depends on the impedance type. Therefore, no general rule for stability criteria can be given for these modes.

Figure 4 for example shows an illustrative view of the mode $l = 1$ together with the SPS resistive wall impedance (decreasing with frequency) and the SPS ferrite loaded kicker impedance (increasing with frequency). For the resistive wall impedance and for $\xi < |\xi_{max}|$ (ξ_{max} is defined as the chromaticity value at which the first sign inversion of the growth rate occurs) the mode $l = 1$ is destabilizing for positive chromaticity and stabilizing for negative chromaticity, the situation is exactly reversed in the case of the impedance of ferrite loaded kickers, which is increasing with frequency up to almost 1 GHz. The overall effect of different impedance contributions depends on the weight of stabilizing and destabilizing effects. An impedance increasing with frequency has a stabilizing effect for mode $l = 1$ and $\xi > 0$. Reducing this kind of impedance makes the situation worse.

A first attempt to understand the nature and the possible impedance source of the instability was performed by using the SPS impedance model [11]. This model was successfully adopted in the past years to benchmark several single bunch beam observations (instability growth rate of mode 0 versus chromaticity [11], tune shift versus intensity and Transverse Mode Coupling Instability (TMCI) behaviour [12]).

The effect of the elements included in the model has been studied and it was found that the combination of kickers and wall impedance is responsible for the observed instability [13].

The expected growth rates as a function of the chromaticity are shown in Fig. 5 for the different modes. The results are in good agreement with the measured intra-bunch motion versus chromaticity [14] discussed in the previous section. This is a strong indication about the nature of the instability, which is considered to be a head-tail instability requiring multiple bunches to be strong enough to be observed in the machine.

Macro-Particle Simulations

The analysis with Sacherer theory allowed the possible nature of the instability and the impedance sources to be identified. However, the development of a macro-particle model for multi-bunch simulations including the actual beam pattern, the feedback system, the detuning impedance and the effect of nonlinear chromaticity, octupoles and nonlinear synchrotron motion is essential to perform quantitative com-

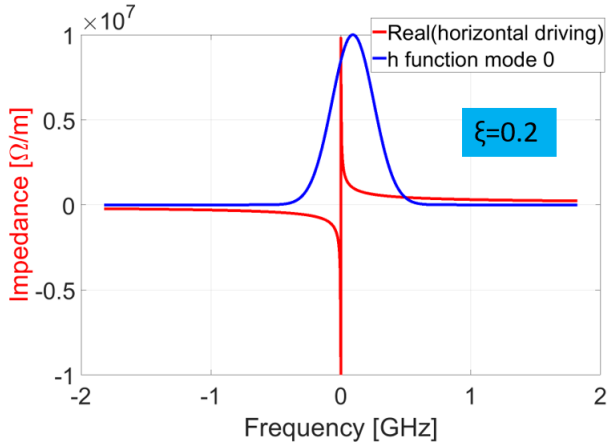

Figure 3: SPS wall impedance model (red) and power spectral density for the mode $l = 0$ in arbitrary units for a chromaticity $\xi = 0.2$ (blue) at injection energy for the Q20 optics.

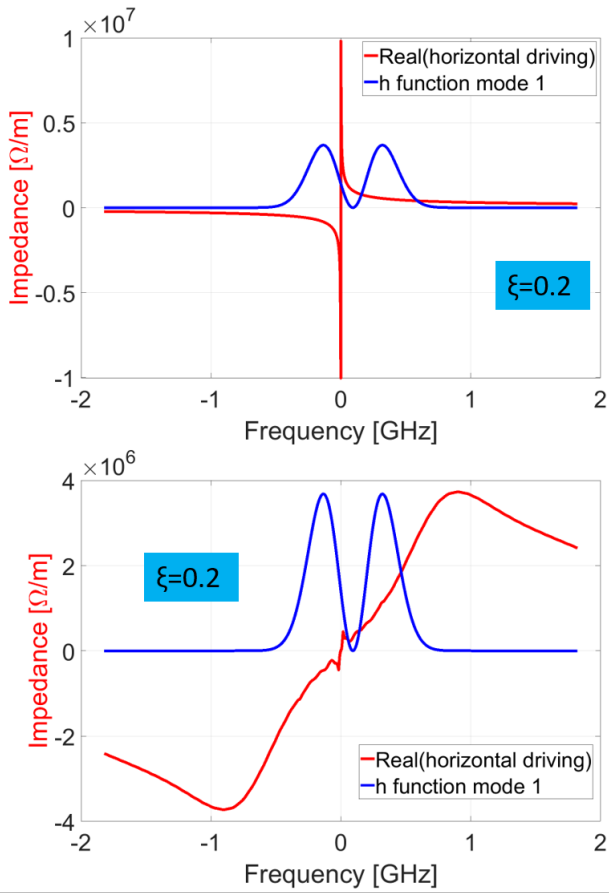

Figure 4: Power spectral density for the mode $l = 1$ in arbitrary units for a chromaticity $\xi = 0.2$ (blue) together with the SPS wall impedance model (top) and the SPS kickers without serigraphy (bottom) at injection energy for the Q20 optics.

ISBN: 978-3-95450-225-7 ISSN: 2673-5571 doi:10.18429/JACoW-HB2021-MOP12

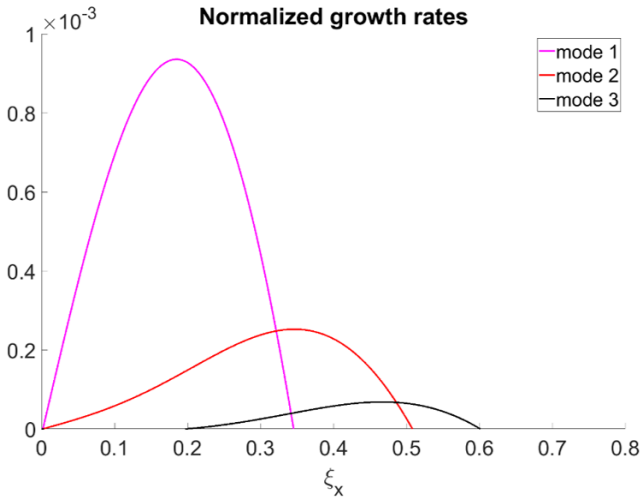

Figure 5: Normalized horizontal instability growth rates as function of the horizontal chromaticity of the head-tail mode 1 in magenta, mode 2 in red and mode 3 in black. The growth rates have been computed by using the Sacherer theory with Gaussian bunches for the SPS impedance model at injection energy for the Q20 optics.

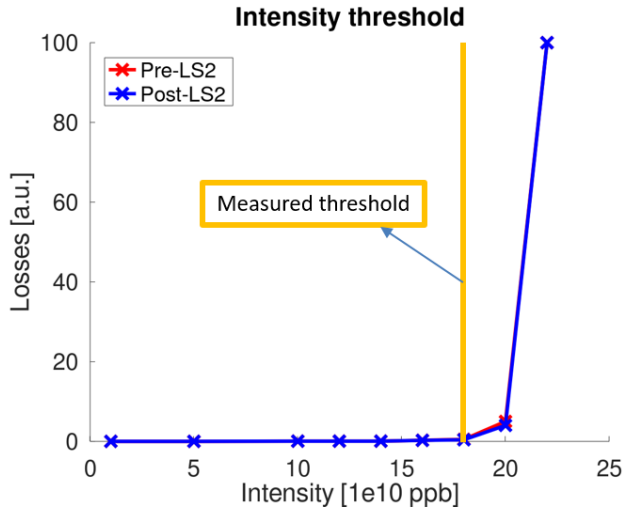

Figure 6: Losses versus intensity. Measured intensity threshold of the instability is represented with the orange line. Both pre-LS2 case (representing the situation during 2018 measurements) and post-LS2 case are displayed, but these two curves are almost indistinguishable as the upgrades of the machine are not expected to change the transverse impedance significantly.

parisons with the measurements. These studies allow the level of accuracy of the model to be qualified, when used to investigate some possible cures of the instability in the unexplored range of intensities. The macro-particle simulations were performed with the multi-bunch version of PyHEADTAIL [15]. The SPS wake model, which is the main input of these simulations, has been successfully benchmarked in past years with single bunch measurements. However, the 10 ns single bunch model is not appropriate for multi-bunch simulations. A big effort has been devoted to the development of a model more appropriate for multi-bunch studies. In particular, the wall wake has been computed up to 1 ms allowing to take into account a wake memory of 43 turns, and the kicker wake has been computed over 1 μs in order to consider all the relevant range of the wake before it vanishes.

The coupled-bunch wake model, including kickers and wall impedance, was then used to benchmark the observation of the SPS horizontal instability with the multi-bunch version of PyHEADTAIL. The simulation considers the exact beam pattern used in measurements (4×48 bunches with 25 ns bunch spacing and a batch gap of 200 ns). An initial Gaussian distribution with $\sigma_z = 0.23$ m is used. A nonlinear model is used for chromaticity (up to the third order) and synchrotron motion. The double SPS RF system is also taken into account and an ideal bunch-by-bunch damper with damping time of 30 turns is included. The initial transverse emittance of the beam is set to 2.5 µm.

The simulations can reproduce the main instability observations such as the bunch intensity threshold (see Fig. 6) and the growth rate versus chromaticity for optimized damper settings (see Fig. 7). The behavior with chromaticity and octupoles of Fig. 2 is also reproduced (see Fig. 8).

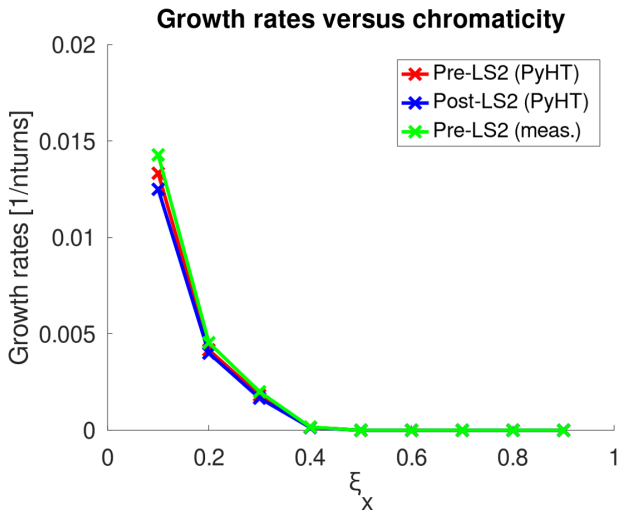

Figure 7: Growth rates as function of the horizontal chromaticity of the instability for a bunch intensity of 2.0×10^{11} ppb. Pre-LS2 and post-LS2 cases have been computed with PyHEADTAIL simulations and compared with the measured values obtained with optimized damper settings.

PREDICTION FOR THE LIU BEAM

The model used in the PyHEADTAIL multi-bunch simulations has reproduced the behaviour of the instability with a high degree of accuracy [16]. The remarkable agreement in the behaviour versus chromaticity and octupoles gave us confidence to use the simulation model to investigate possible stabilization strategies for the nominal LIU beam (4×72 bunches with 2.6×10^{11} ppb at injection) using chromaticity and octupole knobs.

ISBN: 978-3-95450-225-7 ISSN: 2673-5571 doi:10.18429/JACoW-HB2021-MOP12

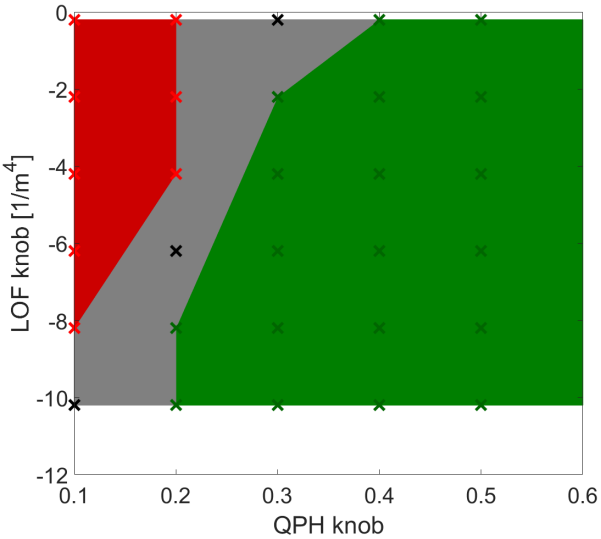

Figure 8: Horizontal beam stability for different chromaticity and octupole settings as obtained from PyHEADTAIL simulations with bunch intensity of 1.8×10^{11} ppb, where the QPH knob controls the normalised horizontal chromaticity ξ_H and the LOF knob controls the normalised octupole strength. The markers indicate unstable (red), stable (green) and settings where there are no significant losses but exponential growth of the amplitude is visible (black). These points could be reasonably assumed to be at the limit of stability.

The simulations are summarized in the stability map displayed in Fig. 9. A simulation point is assumed to be stable if over 10000 SPS turns there is no exponential amplitude growth, emittance blow-up is below 10% and losses are below 1%. Stable points are represented in green and unstable points in magenta. Using these points the unstable area is depicted in red. Stability without octupoles is expected for $\xi_H \geq 0.7$. With octupoles for $|kLOF| < 10$ stabilization is expected for $\xi_H \geq 0.5$. Beam lifetime and quality for the explored operational settings still need to be investigated.

The backup mitigation strategy is the deployment of a wide band feedback system [17]. A prototype of such a system has been demonstrated to be effective in the SPS in the vertical plane against TMCI. Efficiency for the horizontal instability with multiple-bunches needs to be verified in simulation. In order to be able to install the system in the horizontal plane during LS3, dedicated studies need to be launched by 2023. An alternative mitigation strategy could consist in the introduction of an ad-hoc impedance to have a stabilizing effect for the head-tail mode 1-2 horizontal instability [18].

CONCLUSION

The SPS horizontal instability could be a serious limitation to inject the nominal LIU beam (4×72 bunches with N=2.6×10^{11} ppb). The impedance mechanism driving the instability has been identified by using Sacherer theory. A more detailed simulation model including the actual filling scheme, damper, detuning impedance and nonlinearities can reproduce intensity threshold and growth rate versus chromaticity as well as the behaviour of the instability for different settings of octupoles and chromaticity.

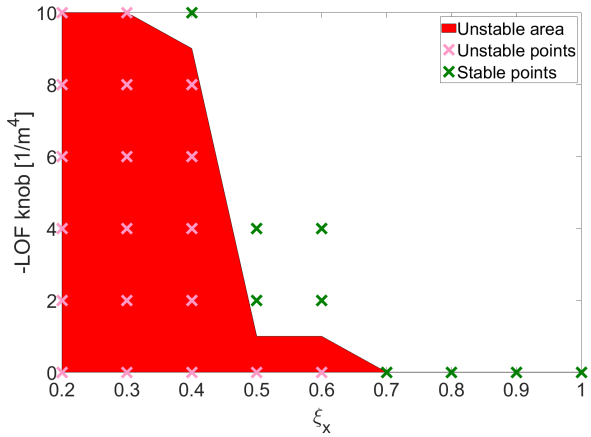

Figure 9: Stability map at injection energy for the nominal LIU beam (4×72 bunches with N=2.6×10^{11} ppb). Stable points are represented in green and unstable points in magenta. Using these points the unstable area is depicted in red. A simulation point is considered to be stable if over 10000 SPS turns there is no exponential amplitude growth, emittance blow-up is below 10% and losses are below 1%.

The simulation model was used to identify a possible stabilization strategy. The simulations predict stabilization of nominal LIU beam for $\xi_H \geq 0.7$ without octupoles and $\xi_H \geq 0.5$ with octupoles. Beam lifetime and quality for the explored settings still need to be investigated.

ACKNOWLEDGMENTS

The authors would like to thank V. Kain and the Operation teams for the continuous support. A special thanks to G. Kotzian and W. Hofle for the optimization of damper settings during measurements, T. Levens for the support with the Head-Tail monitor application and J. Kompulla for the development of the PyHEADTAIL multi-bunch version.

REFERENCES

[1] K. Hanke *et al.*, "The LHC Injectors Upgrade (LIU) Project at CERN: Proton Injector Chain", in *Proc. 8th Int. Particle Accelerator Conf. (IPAC'17)*, Copenhagen, Denmark, May 2017, pp. 3335–3338. doi:10.18429/JACoW-IPAC2017-WEPVA036

[2] H. Bartosik *et al.*, "The LHC Injectors Upgrade (LIU) Project at CERN: Ion Injector Chain", in *Proc. 8th Int. Particle Accelerator Conf. (IPAC'17)*, Copenhagen, Denmark, May 2017, pp. 2089–2092. doi:10.18429/JACoW-IPAC2017-TUPVA020

[3] H. Damerau *et al.*, "LHC Injectors Upgrade, Technical Design Report". CERN, Geneva, Switzerland, Rep. Dec. 2014.

ISBN: 978-3-95450-225-7 ISSN: 2673-5571 doi:10.18429/JACoW-HB2021-MOP12

[4] F. J. Sacherer, "Transverse resistive-wall instabilities of the bunched beam in the SPS," CERN, Geneva, Switzerland, Rep. CERN-SI-NOTE-BR-72-1, May 1972.

[5] B. W. Zotter, "The effective coupling impedance for instabilities of Gaussian bunches," CERN, Geneva, Switzerland, Rep. CERN-ISR-TH-80-03, 1980.

[6] B. W. Zotter, "The effective coupling impedance for bunched beam instabilities," CERN, Geneva, Switzerland, Rep. CERN-ISR-TH-78-16, 1978.

[7] A. W. Chao, *Physics of collective beam instabilities in high energy accelerators*. New York, NY, USA: Wiley, 1993.

[8] B. W. Zotter, "Collective effects: General description," CERN, Geneva, Switzerland, Rep. CERN-85-19-V-2, pp. 415–431, 1984.

[9] J. L. Laclare, "Introduction to coherent instabilities: Coasting beam case," CERN, Geneva, Switzerland, Rep. CERN-85-19-V-2, pp. 377–414, 1985.

[10] J. L. Laclare, "Bunched beam coherent instabilities," CERN, Geneva, Switzerland, Rep. CERN-87-03-V-1, pp. 264–326, 1987.

[11] C. Zannini, H. Bartosik, G. Iadarola, G. Rumolo, and B. Salvant, "Benchmarking the CERN-SPS Transverse Impedance Model with Measured Headtail Growth Rates", in *Proc. 6th Int. Particle Accelerator Conf. (IPAC'15)*, Richmond, VA, USA, May 2015, pp. 402–405. doi:10.18429/JACoW-IPAC2015-MOPJE049

[12] H. Bartosik, G. Iadarola, Y. Papaphilippou, G. Rumolo, B. Salvant, and C. Zannini, "TMCI Thresholds for LHC Single Bunches in the CERN-SPS and Comparison with Simulations", in *Proc. 5th Int. Particle Accelerator Conf. (IPAC'14)*, Dresden, Germany, Jun. 2014, pp. 1407–1409. doi:10.18429/JACoW-IPAC2014-TUPME026

[13] C. Zannini *et al.*, "CERN-SPS horizontal instability: impedance model expectations," Presented at the HSC section meeting, Sep. 2018, https://indico.cern.ch/event/752791/.

[14] C. Zannini *et al.*, "The SPS transverse instability at injection," Presented at the HSC section meeting, Aug. 2019, https://indico.cern.ch/event/940765/.

[15] M. Schenk, "PyHEADTAIL multi-bunch tutorial," Presented at the HSC section meeting, Jan. 2019, https://indico.cern.ch/event/791774/.

[16] C. Zannini *et al.*, "The SPS bunch-by-bunch tune shifts," Presented at the HSC section meeting, Apr. 2021, https://indico.cern.ch/event/129732/.

[17] J. M. Cesaratto *et al.*, "SPS Wideband Transverse Feedback Kicker: Design Report," CERN, Geneva, Switzerland, Rep. CERN-ACC-NOTE-2013-0047, 2013.

[18] C. Zannini *et al.*, "Low impedance design with example of kickers (including cables) and potential of metamaterials," in *Proc. of the ICFA mini-Workshop on Mitigation of Coherent Beam Instabilities in Particle Accelerators (MCBI 2019)*, pp. 167–174, CERN Yellow Reports, Sep. 2020. doi:10.23732/CYRCP-2020-009.167